

# The activity of fused-iron catalyst doped with lithium oxide for ammonia synthesis

Roman Jedrzejewski<sup>1</sup>, Zofia Lendzion-Bieluń<sup>2\*</sup>, Walerian Arabczyk<sup>2</sup>

<sup>1</sup>West Pomeranian University of Technology, Szczecin, Institute of Materials Science and Engineering, Piastów 19, 70-310 Szczecin, Poland

<sup>2</sup>West Pomeranian University of Technology, Szczecin, Institute of Inorganic Chemical Technology and Environmental Engineering, Pułaskiego 10, 70-322 Szczecin, Poland

\*Corresponding author: e-mail: zosi@zut.edu.pl

The iron catalyst precursor promoted with  $\text{Al}_2\text{O}_3$ ,  $\text{CaO}$ , and  $\text{Li}_2\text{O}$  was obtained applying the fusing method. Lithium oxide forms two phases in this iron catalyst: a chemical compound with iron oxide ( $\text{Li}_2\text{Fe}_3\text{O}_4$ ) and a solid solution with magnetite. The catalyst promoted with lithium oxide was not fully reduced at 773 K, while the catalyst containing potassium was easily reducible at the same conditions. After reduction at 873 K the activity of the catalyst promoted with lithium oxide was 41% higher per surface than the activity of the catalyst promoted with potassium oxide. The concentration of free active sites on the surface of the catalyst containing lithium oxide after full reduction was greater than the concentration of free active sites on the surface of the catalyst promoted with potassium oxide.

**Keywords:** iron catalyst, ammonia synthesis, lithium oxide.

## INTRODUCTION

The most commonly used catalyst in the ammonia synthesis is the fused-iron catalyst, in which the main phase is widely described as magnetite<sup>1–4</sup>. In the last years, some articles have shown the catalyst of which the main phase is wustite<sup>5–9</sup>. To expand the surface of the iron catalyst structure, promoters, such as  $\text{Al}_2\text{O}_3$  and  $\text{CaO}$  are added. The addition increases the surface area and prevents from recrystallization of the catalyst<sup>10</sup>. Potassium oxide (the activating promoter) raises the activity of the catalyst, even though it also causes a significant decrease in the specific surface area. According to a double-layer model of the fused iron catalyst for the ammonia synthesis, potassium atoms are bound on the iron surface with oxygen atoms and active sites, on which nitrogen sorption and the ammonia synthesis reaction take place. Active sites are placed under the potassium atom layer<sup>11–12</sup>. Potassium atoms have a significant ability of migration over the iron surface<sup>13</sup>, at the reaction conditions their stability is due to the bond with iron through the oxygen atoms. The authors<sup>14</sup> also assigned potassium to an accelerating role in the ammonia desorption. Explorations of the active sites by wetting the surface of iron catalyst by promoters have been performed in other studies<sup>4, 10, 11</sup>.

Literature studies of the activating effect of promoters on the activity of the catalysts showed that lithium does not activate the surface of the iron catalyst<sup>2, 15–17</sup>. Other studies<sup>18–19</sup> on the influence of alkali metals on the activity of the catalyst in the ammonia synthesis did not cover lithium impact. Nevertheless, studies, in which lithium oxide was introduced into the reduced doubly promoted ( $\text{CaO}$ ,  $\text{Al}_2\text{O}_3$ ) iron catalyst impregnated with lithium hydroxide water solution<sup>20</sup>, has been carried out recently. The activity of catalyst containing 0.79% of  $\text{Li}_2\text{O}$  and reduced at 773 K was similar to the activity of an industrial iron catalyst promoted with potassium oxide. After reduction at 923 K the catalyst containing 0.48% of  $\text{Li}_2\text{O}$  was 15% more active than the industrial catalyst. Increase in  $\text{Li}_2\text{O}$  concentration results in the decrease

of the surface area of the catalyst reduced at 923 K. The most active catalysts promoted with lithium oxide were more active than the industrial catalyst when their activity was calculated and scaled to surface area units.

From the technological point of view, obtaining a catalyst by impregnation requires additional operations. The aim of this work was to check the activity of the fused iron catalyst promoted with  $\text{Li}_2\text{O}$  in the ammonia synthesis. The lithium oxide was introduced into the catalyst precursor by melting with iron oxides and the other oxides of promoters.

## EXPERIMENTAL

Precursors of the catalysts promoted with lithium oxide ( $\text{CAT}_{\text{Li}}$ ) and potassium oxide ( $\text{CAT}_{\text{Ind}}$ ) were obtained in a laboratory installation<sup>21</sup>. The “precursor” refers to the oxidized form of a catalyst. To prepare the catalyst precursors  $\text{CAT}_{\text{Li}}$  and  $\text{CAT}_{\text{Ind}}$ , magnetite ore,  $\text{Al}_2\text{O}_3$ ,  $\text{CaO}$ , and  $\text{LiOH}$  or  $\text{KNO}_3$  were used. In order to obtain the ratio of  $\text{Fe}^{2+}/\text{Fe}^{3+}$  ions similar to industrial catalysts, the iron powder was added as a reducer. The mixture was placed between the water cooled electrodes. A small amount of 2.0–4.5 mm magnetite grains was also placed between the electrodes. With the aid of an additional electrode, melting started progressively, fusing the main path between the electrodes. With the increasing volume of molten mixture the electrical resistance was reduced so the current increased. After exceeding 25 kVA transformer power the voltage was reduced. Following about 45 minutes, the current stabilized, the whole mixture was melted and the lava was placed into a metal vessel. The catalyst precursor was cooled down in the air to the ambient temperature then it was crushed into fraction of 1–1.2 mm. Precursors of catalysts under these conditions were cooled relatively quickly due to their small volumes.

The chemical composition of the catalyst precursors was determined with atomic emission spectroscopy with an inductively-coupled plasma ICP-AES using the Perkin Elmer optical emission spectrometer Optima 5300 DV. The oxidation degree of the samples (expressed as

the mole ratio of  $\text{Fe}^{2+}/\text{Fe}^{3+}$  ions) was determined with well known manganometry method. The phase analysis was determined with the XRD method using a Philips X'Pert Pro with  $\text{Cu K}\alpha$  radiation. This was carried out in HighScore using the ICDD database. The average nanocrystallites size was calculated using the Scherrer equation<sup>22</sup>. Big crystalline iron was used as a reference sample, which reflections showed no broadening associated with the size of crystallites and a distortion network.

The quantitative distribution of promoters in the particular crystallographic phases of the catalyst precursor ( $\text{CAT}_{\text{Li}}$ ) was determined by utilizing the differences in the etching rates of the examined catalyst phases<sup>23</sup>. This was based on the partial dissolution in hydrochloric acid of finely ground catalyst precursor for various periods of time. The resulting solutions were analyzed for element concentrations. From these values, the dependence of the dissolution degree of calcium, aluminum, potassium, and lithium, depending on the dissolution degree of iron, was derived. XRD spectra were taken from the remaining catalysts after each stage of etching. Based on these data, the etching rate of  $\text{Li}_2\text{Fe}_3\text{O}_4$  phase was determined by calculation the quotient of the XRD peak intensity of this phase and the peak intensity of magnetite. Chemical compositions in different phases of the oxidized catalyst were also calculated.

Temperature-programmed desorption processes of hydrogen ( $\text{H}_2$ -TPD) were measured on the AutoChem 2920 instrument (Micrometrics). Catalysts were reduced with the hydrogen at 673 K or 773 K and then purged in Ar gas for 1 h. Sorption of hydrogen was carried out at 25°C for 0.5 h. Desorption of hydrogen was performed in the flow of 40 ml/min of argon with linear gradient of temperature (20°C/min).

The activities of the obtained catalysts in the ammonia synthesis process were measured in a laboratory installation. The ammonia synthesis reactor was a six-channel integral reactor with a centrally-located reaction gas feed. The reactor construction ensures good gas mixing, restricts the influence of the external diffusion and dispersion effects typical for pipe reactors. The reduction and synthesis gas was stoichiometric  $\text{N}_2 : 3\text{H}_2$ , obtained from decomposition of  $\text{NH}_3$ . Gaseous ammonia was passed through the preliminary ammonia dryer filled with a mixture of KOH and  $\text{K}_2\text{O}$ . Following this, ammonia was decomposed to the hydrogen-nitrogen mixture by a set of decomposers filled with  $\text{Ni}/\text{Al}_2\text{O}_3$  catalyst operating at 973 K. The obtained mixtures were further dried using silica gel dryers and molecular sieves. At the end of the purifying process the mixture was passed through a reduced iron catalyst under 0.2 MPa (where ammonia synthesis does not occur) to adsorb the remaining poisons over catalyst surface.

Reduction of catalysts was carried out at the pressure of 0.2 MPa under the load 20 000  $\text{h}^{-1}$  according to the procedure: 473 K-1 h, 623 K-2 h, 673 K-12 h, 723 K-24 h, 773 K-24 h. In the last stage, reduction run out under the pressure of 10 MPa at 773 K until the ammonia concentration in the exhaust gases was constant (about 4 h). In order to reduce the catalysts promoted with lithium oxide completely the catalysts were heated at 873 K for 17 h. The activity of the catalysts was measured

under the pressure of 10 MPa at the temperatures of 673, 723, and 773 K.

The catalytic activity expressed as the reaction rate constant was calculated from the integral form of Temkin-Pyzhev<sup>24</sup> equation processed by Kuznecov<sup>2</sup>:

$$r = k \cdot (0.75)^{1.5} \cdot p^{-0.5} \frac{(1-Z)^{2.5}}{Z} \left[ \frac{(Z^r)^2}{(1-Z^r)^4} - \frac{Z^2}{(1-Z)^4} \right]$$

Where:

$r$  – is reaction rate,  $k$  – is reaction rate constant,  $Z$  – is the molar fraction of ammonia at the reactor outlet,  $Z^r$  – is the molar fraction of ammonia in the condition of chemical equilibrium,  $p$  – is synthesis pressure.

The catalysts were unloaded from the ammonia synthesis reactor after reduction at 773 K and 873 K in a nitrogen–hydrogen atmosphere to avoid passivation. The specific surface area was measured with the Micromeritics ASAP 2010 apparatus according to the assumptions of the BET method.

## RESULTS

Chemical content of the catalyst precursors and molar ratio  $\text{Fe}^{2+}/\text{Fe}^{3+}$  is shown in Table 1.

**Table 1.** Chemical content of the catalyst precursors and the mole ratio of  $\text{Fe}^{2+}/\text{Fe}^{3+}$  ions

Name of catalyst	Content [%]				$\text{Fe}^{2+}/\text{Fe}^{3+}$
	$\text{Al}_2\text{O}_3$	CaO	$\text{K}_2\text{O}$	$\text{Li}_2\text{O}$	
$\text{CAT}_{\text{Li}}$	3.33	0.84	–	0.96	0.63
$\text{CAT}_{\text{Ind}}$	2.31	2.94	0.53	–	0.65

Figure 1 shows the XRD patterns of the industrial catalyst precursor ( $\text{CAT}_{\text{Ind}}$ ) and the precursor of the catalyst promoted with lithium oxide ( $\text{CAT}_{\text{Li}}$ ).

The main phase of both catalyst precursors was  $\text{Fe}_3\text{O}_4$ . In the catalyst precursor promoted with potassium oxide (Fig. 1.  $\text{CAT}_{\text{Ind}}$ ),  $\text{CaFe}_3\text{O}_5$  phases were identified as well as FeO. The XRD pattern of the catalyst precursor promoted with lithium oxide (Fig. 1.  $\text{CAT}_{\text{Li}}$ ) showed that beside the  $\text{Fe}_3\text{O}_4$  phase, there was also an  $\text{Li}_2\text{Fe}_3\text{O}_4$  phase (ICDD 37-1432).  $\text{Li}_2\text{Fe}_3\text{O}_4$  crystallized similarly as  $\text{Fe}_3\text{O}_4$  in a cubic crystal system with the same space group, Fd-3 m, and space group number 227. Although there was an excess of  $\text{Fe}^{2+}$ , a wustite phase, in the contrary to the  $\text{CAT}_{\text{Ind}}$  catalyst promoted with potassium oxide, was not identified. Excess  $\text{Fe}^{2+}$  created a phase with  $\text{Li}_2\text{O}$ .

After the reduction of both catalysts precursors at 873 K, only the iron phase was identified (Fig. 2).

The selective etching method, described in details in the paper<sup>23</sup> was used to determine the distribution of the promoters in the catalyst promoted with lithium addition. Analyzing the dependence of the etching degree of promoters on the etching degree of iron in the catalyst precursor promoted with lithium oxide (Fig. 3), it was observed that 100% of lithium oxide was etched with the etching of iron so that it is bound with iron oxides.

After etching of 60% of iron only the magnetite phase remained in the catalyst. It was stated on the basis of X-ray analysis. From the etching line slope (dashed line) it was found that 14% of total lithium oxide was bound with iron as magnetite. On the basis of total lithium content in the catalyst and lithium amount bound with

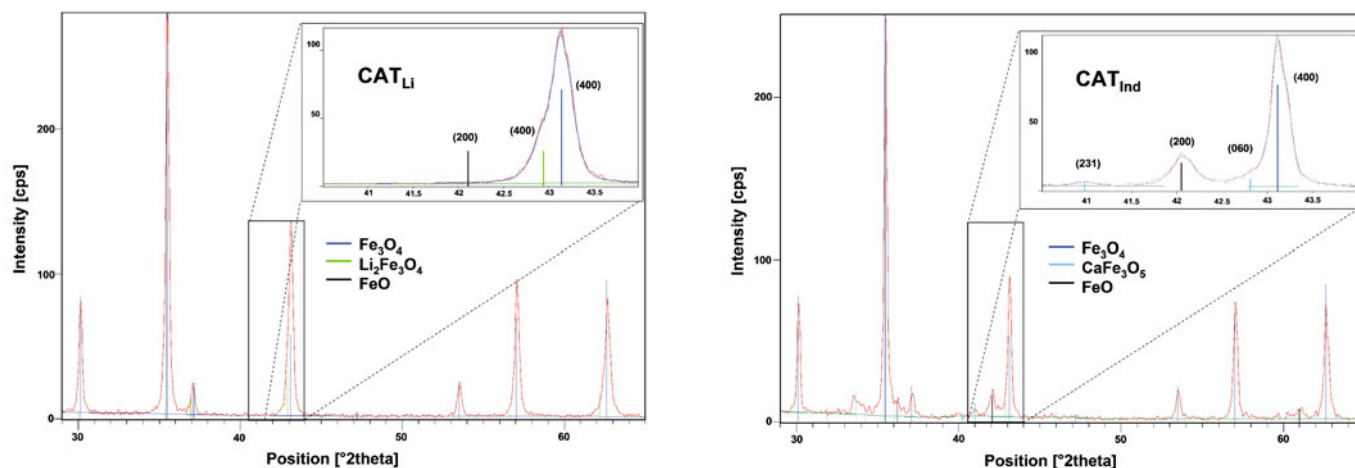


**Figure 1.** XRD spectra of the fused iron catalyst precursor promoted with potassium oxide  $CAT_{Ind}$  and promoted with lithium oxide  $CAT_{Li}$

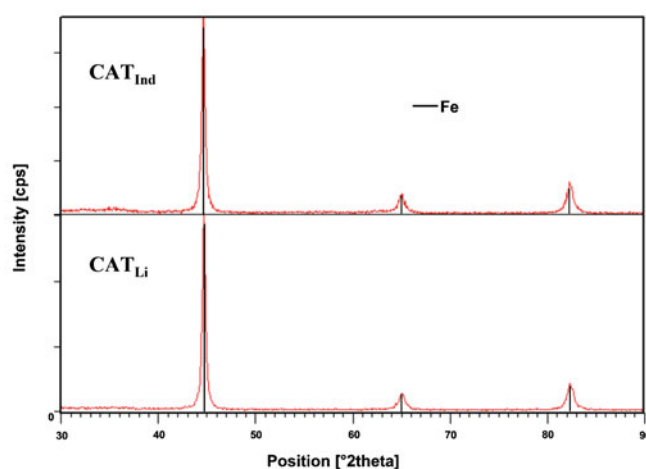


**Figure 2.** XRD spectra of the iron catalysts after the activity test

magnetite lithium oxide concentration in magnetite was calculated as 0.13 wt%. The rest of lithium oxide, 86%, is bound with iron and forms the  $Li_2Fe_3O_4$  phase. The solid phase of the catalyst at various etching degrees was examined with an aid of XRD method.

Changes of the ratio of peaks intensities of  $Li_2Fe_3O_4$  and  $Fe_3O_4$  phases with rising etching degree are shown in Figure 3. The phase containing lithium was etched faster in comparison to pure magnetite. On the basis of the calcium etching curve it may be concluded that around 50% of the calcium oxide was located in the intergranular spaces not bound with iron. The  $CaFe_3O_5$  phase was not identified, so the calcium oxide connected with iron in the intergranular spaces did not occur. The rest of the calcium oxide created a solid solution with magnetite. To form  $CaFe_3O_5$  in precursors of the fused catalysts promoted with lithium oxide CaO must be present in appropriate concentration. Aluminium oxide in  $CAT_{Li}$  was distributed in the same way as in the industrial iron catalyst<sup>23</sup>. More than 90% of total amount of  $Al_2O_3$  was built in into magnetite. Comparing the presented distribution of promoters in the structure of  $CAT_{Li}$  precursor promoted with lithium oxide with the distribution of promoters in  $CAT_{Ind}$  precursor promoted with potassium<sup>23</sup> oxide there are significant differences in location of these oxides, lithium and potassium oxides respectively. In all investigated catalyst<sup>25-26</sup>, in which molar ratio of  $Fe^{2+}/Fe^{3+}$  was higher than 0.5, potassium oxide

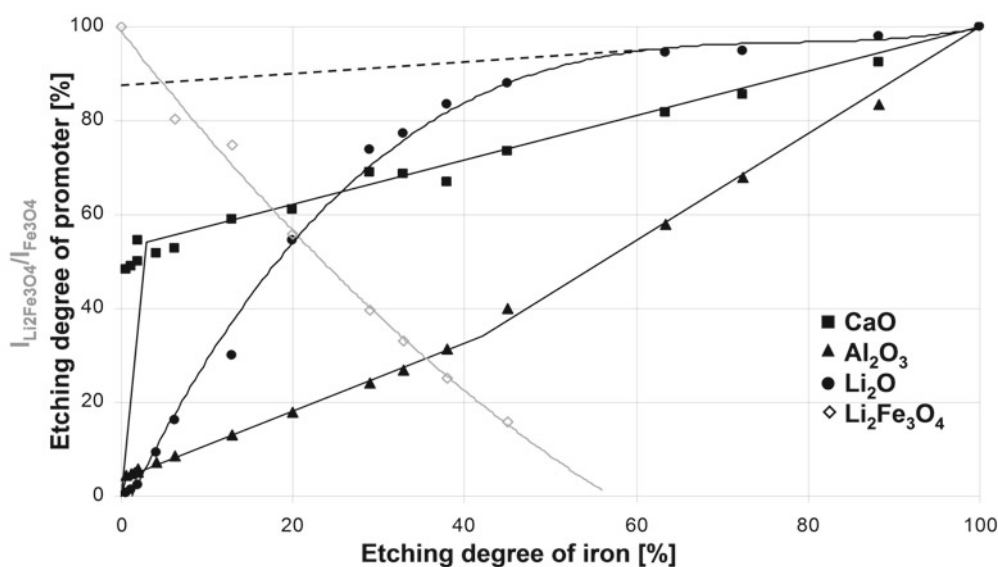


**Figure 3.** The relationship between the calcium, aluminium, and lithium oxide etching degrees and the etching degree of iron in the  $CAT_{Li}$  precursor. Line corresponds to the lithium oxide content in magnetite was extended by the dashed line. The etching rate of  $Li_2Fe_3O_4$  phase was determined by the XRD method and expressed as an intensity ratio of  $I_{Li_2Fe_3O_4}/I_{Fe_3O_4}$

in the amount of more than 90% is not bound with iron oxide and it may be washed with water. Lithium oxide is bound with iron oxides.

The catalyst activity in the ammonia synthesis reaction (expressed by the rate constant  $k$  of Tiemkin-Pyzhev equation) is present in Figure 4 as the Arrhenius function. The activity of the obtained catalyst  $CAT_{Li}$  promoted with lithium oxide was compared with the activity of the catalyst ( $CAT_{Ind}$ ) promoted with potassium oxide. The comparison of the activity of the catalyst promoted with lithium oxide, introduced using the impregnation method and a content of lithium oxide of  $X_{Li_2O} = 12 \text{ mmol} \cdot \text{mol}^{-1}$ <sup>20</sup>, with the activity of the catalysts  $CAT_{Li}$  and  $CAT_{Ind}$  was additionally presented in Figure 4.

The activity of the catalyst  $CAT_{Li}$  promoted with lithium oxide is lower in comparison with the activity of the catalyst  $CAT_{Ind}$  promoted with potassium oxide both after reduction at 773 K and at 873 K. The activity of the catalyst impregnated with lithium oxide is comparable with the activity of the  $CAT_{Ind}$  catalyst. It is worth to be noticed that the activity of the catalyst promoted with lithium oxide increased after reduction at 873 K in comparison to the activity after reduction at 773 K. The catalyst promoted with potassium behaved differently. Its activity dropped down after reduction at 873 K.

The table below shows the reaction rate constants per weight of the catalyst ( $k$ ) and per specific surface area of the catalyst ( $k_1$ ) at 773 K after reduction at the temperature of 773 K and 873 K.

Comparing  $CAT_{Li}$  catalyst activity at 773 K given as a reaction rate constant for mass of the catalyst ( $k$ ), one should state that increase in reduction temperature makes increase in the activity of 44%. For catalyst promoted with potassium decrease of activity of 16% was observed. The specific surface area of the catalysts

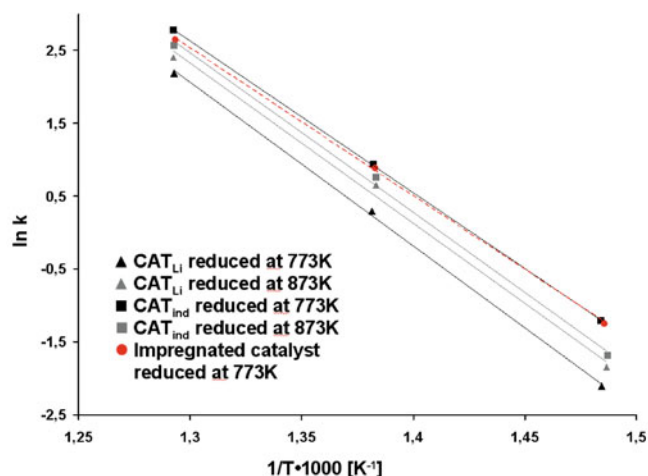


Figure 4. Dependence of the rate constant as a function of temperature for the sample after reduction at 773 K and 873 K

Table 2. Characteristic of catalysts

Name / reduction temperature	S	d	$N_{ad}$	k	$k_1$
	[m <sup>2</sup> /g]	[nm]	[cm <sup>3</sup> /m <sup>2</sup> ]	[g <sub>NH<sub>3</sub></sub> · MPa <sup>0.5</sup> /g · h]	[g <sub>NH<sub>3</sub></sub> · MPa <sup>0.5</sup> /m <sup>2</sup> · h]
CAT <sub>Li</sub> / 773K	27.5	10	0.0146	1.34	0.048
CAT <sub>Li</sub> / 873K	5.4	21	0.0603	1.93	0.357
CAT <sub>Ind</sub> / 773K	17.0	20	0.0204	2.56	0.150
CAT <sub>Ind</sub> / 873K	8.5	36	0.0318	2.15	0.253

S – specific surface area, d – average crystallite size of iron,  $N_{ad}$  – the relative number of adsorption sites.

decreased after reduction at 873 K.  $CAT_{Li}$  was not fully reduced at 773 K where the  $CAT_{Ind}$  was reduced. The fused catalyst promoted with lithium oxide required higher reduction temperatures, what caused significant decreases of the specific surface areas because of the large recrystallization.

After reduction at 873 K, the  $CAT_{Li}$  catalyst had an activity per surface 41% higher than the  $CAT_{Ind}$  catalyst. Catalyst activity depends on an active surface which measure is a number of active sites over that a reaction takes place. As a result of deep reduction ( $T_{red} = 873 \text{ K}$ ), the recrystallization process occurred, what caused a significant decrease in the specific surface area. Although on the basis of the increase in catalyst activity it can be concluded that the number of active sites on the surface of the catalyst  $CAT_{Li}$  increased.

Figure 5 shows the TPD- $H_2$  curves for catalysts after reduction at 773 K and 873 K. There are three visible peaks on the curve what indicates the presence of three adsorption states. However according to previous investigations<sup>27</sup> only the first peak, marked  $\alpha_1$ , is connected with the hydrogen adsorption over the catalyst surface. Remaining peaks relate to hydrogen desorption, which is dissolved in the catalyst. Calculating surface area under the peak  $\alpha_1$  the volume of surface bound hydrogen was found. On the basis of hydrogen volume and the total surface area the relative number of active sites ( $N_{ad}$ ) on the catalyst surface as a function of the reduction temperature of the catalyst precursors were determined, Table 2.

The decrease in the specific surface area was observed while the reduction temperature rose.

But the relative number of active sites, expressed as a ratio of adsorbed hydrogen and specific surface area, rises while the reduction temperature rises. It is particularly visible for the catalyst promoted with lithium oxide.

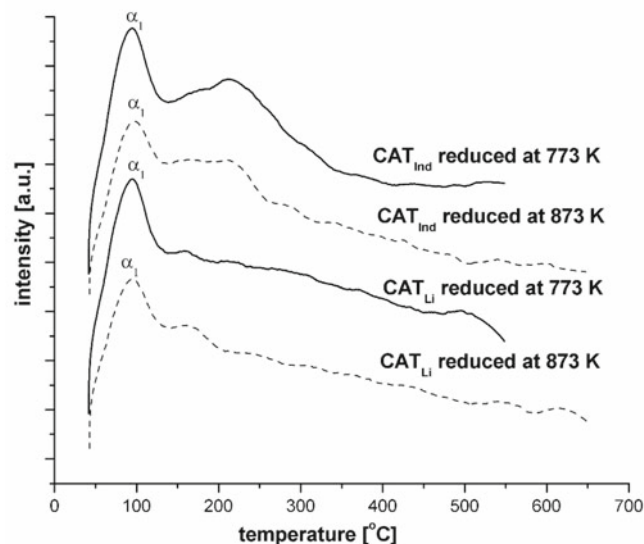
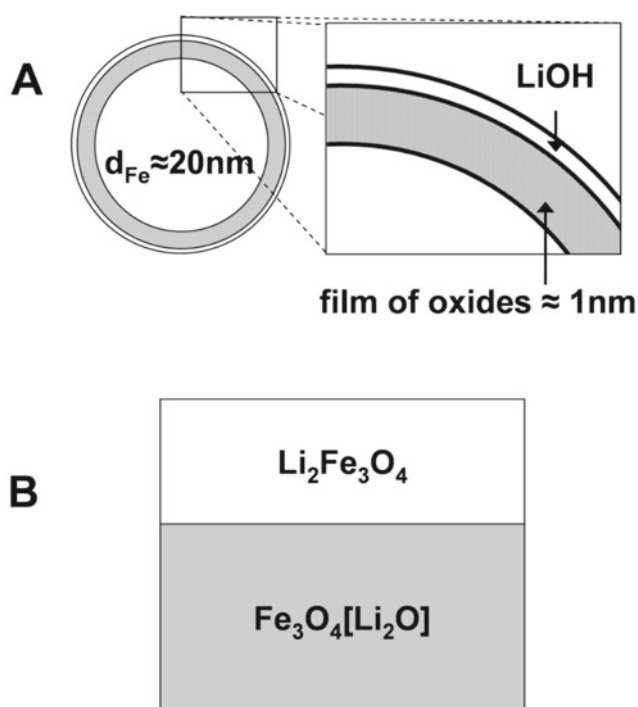


Figure 5.  $H_2$ -TPD spectra for the catalysts

According to the worked out model of the double layer iron catalyst<sup>11</sup> there is the dependence between catalyst active surface, formed by active sites, and promoters, especially potassium. Potassium takes part in the free adsorption sites formation, over which chemical reaction occurs. Lithium and potassium belong to the same group of elements but lithium action during catalyst structure forming is completely different. During a catalyst melting process lithium combines totally with iron as a solid solution in the magnetite phase and as the  $\text{Li}_2\text{Fe}_3\text{O}_4$  phase (Fig. 3). Contrary to lithium, potassium, at the amount of over 90%, is located in the boundary spaces and it is not combined with iron. In the reduction process of the iron catalyst with potassium, potassium oxide wets formed iron crystals by combining with oxygen. It was confirmed that a change in potassium content in the catalyst impacts on number of adsorption sites what leads to a change in the catalyst activity. Whereas lithium is combined with hard-reducible iron. So lithium does not take part in forming of active adsorption sites on the catalyst surface. Higher reduction temperature is necessary to realise lithium but in that case recrystallization and sintering processes take place what results in decreasing of the catalyst specific surface area.

There is a different situation with the iron catalyst promoted with lithium in the impregnation process. Impregnated catalysts promoted with lithium oxide were more easily reducible than the fused  $\text{CAT}_{\text{Li}}$ <sup>20</sup>. The reduced form of the catalyst, with a well developed structure and passivated surface – covered with thin oxide-layer, was impregnated. Iron crystallites of 20 nm, covered with thin, approximately 1 nm, oxide-layer containing lithium, form the structure of the catalyst (Fig. 6A). In the reduction process, the reaction between  $\text{LiOH}$  and the thin film of oxides occurs. In the fused catalyst (Fig. 6B), the reduction run in the bulk of solid solution lithium oxide in the magnetite and  $\text{Li}_2\text{Fe}_3\text{O}_4$  phases. In



**Figure 6.** Distribution of lithium oxide in A – impregnated catalyst, B – fused catalyst

this stage the structure was formed and the wetting of surfaces by promoters occurred. Specific surface area of the pre-reduced catalyst and then impregnated was significantly higher than – specific surface area of the catalyst oxidized form ( $S_{\text{Fe}} \gg S_{\text{Fe}_3\text{O}_4}$ ). Surface lithium concentration in the  $\text{CAT}_{\text{Li}}$  reduction process is significantly lower.

Depending on the preparation method, lithium oxide had been distributed variously, what caused differences in activity and in the reduction process.

Bearing in mind that there are more active sites on the surface of catalysts promoted with lithium on the surface of catalyst promoted with potassium oxide, there is a promise that a catalyst with properties no worse than the catalysts used currently in industry can be obtained by optimizing the chemical composition and the conditions of catalyst reduction.

## CONCLUSIONS

In fused iron catalysts promoted with lithium oxide, in contrary to potassium oxide (which is not connected with iron oxide and is found in the glass phase in the intergranular spaces), lithium oxide creates a  $\text{Li}_2\text{Fe}_3\text{O}_4$  phase and a solid solution with magnetite. In catalysts obtained using the impregnation method of pre-reduced double-doped ( $\text{Al}_2\text{O}_3$ ,  $\text{CaO}$ ) iron catalysts, the lithium oxide does not create a crystallographic phase detected by the XRD method.

In precursors of catalysts (fused and impregnated) promoted with lithium oxide, the reduction process is more difficult. To complete the reduction a higher temperature is required. At this stage of the optimization of catalyst preparation conditions, the iron catalysts promoted with  $\text{Al}_2\text{O}_3$ ,  $\text{CaO}$ ,  $\text{Li}_2\text{O}$  are obtained:

by the impregnation method, which achieved an activity similar to that of the industrial catalysts used currently,

by fusing iron oxides with oxides of promoters, the activity is 25% lower than the activity of the industrial catalyst.

The concentration of free active sites on the surface of the catalysts containing lithium oxide is greater than the concentration of free active sites on the surface of the catalysts promoted with potassium oxide.

## LITERATURE CITED

- Jennings, J.R. (1991). Catalytic Ammonia Synthesis: Fundamentals and Practice. Plenum Press. New York.
- Kuznieciov, L.D., Dmitrienko, L.M., Rabina, P.D. & Sokolinski, U.A. (1982). Sintiez Ammiaka. Chimia, Moscow.
- Aika, K. & Tamaru, K., in: Nielsen, A. (Ed.). (1995). Ammonia. Catalysis and Manufacture, Springer Verlag, Berlin.
- Ertl, G. (2009). Reactions at Solid Surfaces. Wiley, US
- Liu, H., Xu, R., Jiang, Z., Hu, Z., Li, Y. & Li, X. (1996). US Patent 5, 846, 507 (2002) Europea Patent. 0,763,379 and (2002) Germany Patent 69430143T2.
- Liu, H.Z., Li, X.N. & Hu, Z.N. (1996) Development of novel low temperature and low pressure ammonia synthesis catalyst. Appl. Catal. A. 142, 209–222. DOI: 10.1016/0926-860X(96)00047-6.
- Liu, H.Z. & Li, X.N. (1997). Relationship between Precursor Phase Composition and Performance of Catalyst for Ammonia Synthesis. Ind. Eng. Chem. Res. 36, 335–342. DOI: 10.1021/IE960072S.

8. Pernicone, N., Ferrero, F., Rossetti, I., Forni, L., Canton, P., Riello, P., Fagherazzi, G., Signoretto, M. & Pinna, F. (2003). Wustite as a new precursor of industrial ammonia synthesis catalysts. *Appl. Catal. A*. 251, 121–129. DOI: 10.1016/S0926-860X(03)00313-2.
9. Lendzion-Bieluń, Z., Arabczyk, W. & Figurski, M. (2002). The effect of the iron oxidation degree on distribution of promoters in the fused catalyst precursors and their activity in the ammonia synthesis reaction. *Appl. Catal. A*. 227, 255–263. DOI: 10.1016/S0926-860X(01)00938-3.
10. Ertl, G., in: Jennings, J.R. (Ed.). (1991). *Catalytic Ammonia Synthesis: Fundamentals and Practice*. Plenum Press. Chapter 3. New York.
11. Arabczyk, W., Narkiewicz, U. & Moszyński, D. (1999). Double-Layer Model of the Fused Iron Catalyst for Ammonia Synthesis. *Langmuir* 15(18), 5785–5789. DOI: 10.1021/la981132x.
12. Ertl, G. & Vac, J. (1983). *Sci. Technol. A1* (2), 1247–1253.
13. Arabczyk, W., Narkiewicz, U. & Moszyński, D. (1999). Influence of potassium/oxygen layer on properties of iron surfaces. *Appl. Catal.* 182, 379–384. DOI: 10.1016/S0926-860X(99)00034-4.
14. Strongin, D.R., Somorjai, G.A. & Catal, J. (1988). The effects of potassium on ammonia synthesis over iron single-crystal surface. *J. Catal.* 10, 951–960. DOI: 10.1016/0021-9517(88)90184-4.
15. Mross, W.D. (1983). Alkali doping in heterogeneous catalysis. *Catal. Rev. Sci. Eng.* 25(4) 591–637.
16. Aleksicz, B., Mitov, J.G., Klisurski, D.G., Pietranowicz N.A., Jovanovic, N.N., Bogdanov, S.S. (1984). Comparative investigations of the effect of alkaline promoters on the activity of ammonia synthesis catalysts at atmospheric and elevated pressures. *Glas. Hem. Drus. Beograd.* 49, 477–483.
17. Bosch, H., Van Omen, J.G., Gellings, P.J. (1985). On the role of alkali metals in ammonia synthesis. *Appl. Catal.* 18, 405–408. DOI:10.1016/S0166-9834(00)84017-8.
18. Rarog, W., Kowalczyk, Z., Sentek, J., Skladanowski, D. & Zielinski, J. (2000). Effect of K, Cs and Ba on the kinetics of NH<sub>3</sub> synthesis over carbon-based ruthenium catalysts. *Catal. Lett.* 68, 163–168.
19. Aika, K. & Shimazaki, K. (1985). Support and promoter effect of ruthenium catalyst I. Characterization of alkali-promoted ruthenium/alumina catalysts for ammonia synthesis. *J. Catal.* 92, 296–304. DOI: 10.1016/0021-9517(85)90264-7.
20. Arabczyk, W., Jasinska, I. & Jędrzejewski, R. (2009). Iron catalyst for ammonia synthesis doped with lithium oxide. *Catal. Comm.* 10, 1821–1823. DOI: 10.1016/j.catcom.2009.06.003.
21. Arabczyk, W., Ziebro, J., Kałucki, K., Świerkowski, R. & Zakrzewska, M. (1996). Laboratory scale plant for continuous fusing of iron catalysts. *Chemik* 1, 22–24. (In Polish).
22. Uvarov, V. & Popov, I. (2007). Metrological characterization of X-ray diffraction methods for determination of crystallite size in nano-scale materials. *Mater. Charac.* 58, 883–891. DOI: 10.1016/j.matchar.2006.09.002.
23. Arabczyk, W. & Lendzion-Bieluń, Z. (2001). Method for determination of the chemical composition of phases of the iron catalyst precursor for ammonia synthesis. *Appl. Catal.* 207, 37–41. DOI: 10.1016/S0926-860X(00)00614-1.
24. Tiemkin, M. & Pyzew, W. (1939). Kinetics of the synthesis of ammonia on promoted iron catalysts. *Phys. J. Chem.* 13, 851. USSR.
25. Lendzion-Bieluń, Z., Arabczyk, W. & Figurski, M. (2002). The effect of the iron oxidation degree on distribution of promoters in the fused catalyst precursors and their activity in the ammonia synthesis reaction. *Appl. Cat.* 227, 255–263. DOI: 10.1016/S0926-860X(01)00938-3.
26. Figurski, M.J., Arabczyk, W., Lendzion-Bieluń, Z. & Lenart, S. (2004). Investigation of manganese-doped iron ammonia synthesis catalysts. *Appl. Cat.* 266(1), 11–20. DOI: 10.1016/j.apcata.2004.01.032.
27. Arabczyk, W., Jasińska, I. & Pelka, R. (2011). Measurements of the relative number of active sites on iron catalyst for ammonia synthesis by hydrogen desorption. *Catal. Today* 169, 97–101. DOI: 10.1016/j.cattod.2010.09.003.